

# Fabrication of Ti/TiO<sub>x</sub> tunneling barriers by tapping mode atomic force microscopy induced local oxidation

B. Irmer, M. Kehrle, H. Lorenz, and J. P. Kotthaus

*Sektion Physik, Ludwig-Maximilians Universität München, 80539 München, Germany*

(Received 2 April 1997; accepted for publication 28 July 1997)

We use an atomic force microscope operating in a dynamic modus, commonly called tapping mode, to completely oxidise through thin 5 nm titanium films using the very local electric field between the tip and the sample. Tapping mode local oxidation minimizes tip degradation and therefore enhances resolution and reliability. By working under a controllable environment and measuring the resistance *in situ* while oxidising we are able to fabricate well-defined isolating Ti–TiO<sub>x</sub>–Ti barriers as small as 15 nm. Their conductance shows an exponential dependence on the oxide width, thereby identifying tunneling as the dominant conduction mechanism. From the nonlinear current-voltage characteristic a tunneling barrier height of 178 meV is derived. © 1997 American Institute of Physics. [S0003-6951(97)01938-4]

The fabrication and study of nanoelectronic devices demands the modification of metals and semiconductors on the nanometer length scale. Key elements for more complex structures such as transistors are narrow conducting wires and, for the single electron transistor (SET) especially, tunneling barriers. They are, however, difficult to define by standard lithographic tools like optical or electron beam lithography. On the nanometer scale proximal probe based instruments, in particular the scanning tunneling microscope (STM) and atomic force microscope (AFM), have proven successful not only to image surfaces but also to modify them.<sup>1</sup> Various approaches have been used to generate patterns useful for device fabrication: mechanically modifying a resist layer that then acts as an etch mask for pattern transfer,<sup>2</sup> local anodic oxidation and subsequent use of the oxide as the etch mask,<sup>3</sup> and maskless techniques, i.e., those directly affecting the material's electron system by the proximal probe itself.<sup>4</sup> This can be done again mechanically<sup>5</sup> or by using the probe for locally inducing chemical reactions. Early work on STM and contact AFM induced oxidation of Si was done by Dagata *et al.*<sup>6</sup> and by Snow *et al.*<sup>3,7</sup> Subsequently, Lyding *et al.*<sup>8</sup> worked under ultrahigh vacuum conditions demonstrating a resolution for surface modifications of better than 10 Å. Oxidation is possible to almost all non-noble materials like Ti,<sup>9</sup> Al,<sup>10</sup> Cr,<sup>11</sup> and GaAs.<sup>6</sup> Yet, the question as to whether metal-oxide-metal junctions prepared by proximal probe techniques are indeed tunneling barriers remains unanswered.

Here, we report on the use of dynamic AFM, also commonly known as tapping mode AFM (TMAFM),<sup>12</sup> induced local oxidation to produce Ti–TiO<sub>x</sub>–Ti barriers and characterize them as tunneling barriers. First 5 nm Ti is thermally evaporated onto 250 nm thick thermally grown SiO<sub>2</sub> layers on a Si substrate. The 1 μm wide wires are predetermined by optical lithography. Following etching in HF, Au bond pads are prepared and electrical leads attached. Finally the device is transferred to the AFM. All modifications are done in a controlled environment by transferring the AFM into a vacuum chamber ( $p=4\times 10^{-4}$  mbar). For wet anodic oxidation the chamber is filled with pure nitrogen bubbling through deionised water. By mixing dry and humid nitrogen streams the humidity level within the chamber can be ad-

justed to levels from 0% to 95%. All AFM modifications and measurements shown here were done at room temperature and in an oxygen free atmosphere with 50% relative humidity. By field oxidising completely through the Ti film, metallic constrictions, metallic channels and the isolating barrier itself are defined. This is controlled by *in situ* electrical measurements that monitor the oxidation.<sup>13</sup>

A limiting factor in AFM lithography is the tip quality. To obtain high resolution the tip radii have to be as small as possible. Conversely, the tip has to be sufficiently conductive. We use commercially available tips made from n-type highly doped silicon,<sup>14</sup> that we additionally sharpen by thermal oxidation and subsequent HF etching.<sup>15</sup> These tips can be biased directly without any conductive film coating. AFM probes, especially those made from single crystal silicon, tend to degrade rapidly during local oxidation due to the additional electrostatic forces. Typically voltages up to 10 V are applied; these voltages are sufficient to scratch away the written pattern when working in contact mode<sup>16</sup> and to blunt the tip.

To overcome this problem, we work in a dynamic AFM mode (TMAFM). The cantilever oscillates near its resonance frequency ( $\approx 300$  kHz) with a high amplitude (up to 100 nm). For oxidation a positive voltage is applied to the substrate (anodic oxidation), resulting in the oxide growing under the negatively biased tip. The electric field forces the cantilever to bend towards the substrate (inset in Fig. 1).<sup>17</sup> As the feedback is operating all the time, the mean tip–sample distance is increased to maintain constant amplitude; see Fig. 1a. No changes in amplitude are observed [Fig. 1(b)], which means, that the tip–sample force is as low as in imaging mode, i.e. several orders of magnitude lower than in contact mode.<sup>12</sup> This contrasts with the work of Servat *et al.*,<sup>18</sup> in which no oxidation was observed for amplitudes larger than 0.1 nm. By taking advantage of the reduced damage to the tip and substrate in TMAFM during *imaging and modification*, we are able to use very fine and therefore fragile tips and maintain their performance during device fabrication. This enhances the resolution and reliability of this technique. To date, oxide lines down to 70 Å in linewidth have been prepared.

Another aspect of TMAFM local oxidation is the short

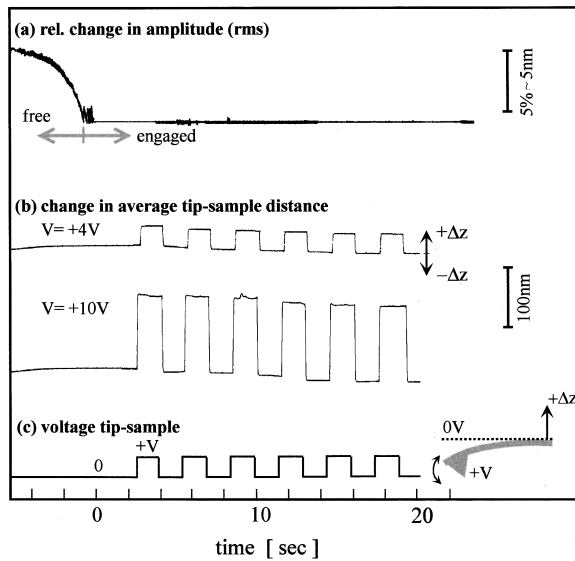


FIG. 1. Influence of an applied voltage in tapping mode AFM: There are no changes in amplitude (a) and therefore no additional forces can be seen if square wave voltage pulses ( $T \approx 4$  s) are applied (c) as the feedback loop re-adjusts the tip-sample distance (b). The initial reduction of  $\approx 5$  nm of the amplitude compared to the free oscillation is due to going into normal scanning mode ( $V=0$ ).

contact time of less than  $10^{-6}$  s between the tip and the water/sample surface. This is too short to explain TMAFM local oxidation in an electrochemical picture where the tip is the cathode and the sample the anode, with water being the electrolyte. Furthermore, the current flow between tip and sample<sup>19</sup> is zero within experimental resolution. We therefore conclude that there is field enhanced aqueous corrosion.

In the first oxidation step the  $1 \mu\text{m}$  wire is constricted to 70 nm. The barrier is then formed by repeatedly scanning across the constriction. The written pattern can easily be seen since the oxide varies in its density  $\rho$  and atomic weight  $M$  from the initial Ti. Assuming the amount of Ti substance that is to be conserved, the change in topography is estimated to be  $d_{\text{TiO}_2}/d_{\text{Ti}} = \rho_{\text{Ti}}/\rho_{\text{TiO}_2} \times M_{\text{TiO}_2}/M_{\text{Ti}}$ . For a 5 nm thin Ti film the oxide extrusion is expected to be  $\approx 3$  nm high. Fig. 2(a) shows a cross section through a typical barrier, derived from two AFM line scans. First the upper part was scanned, then the oxide was removed by etching. The second scan shows a 1.8 nm deep trench, indicating oxide growth into the substrate.<sup>20</sup> In order to thoroughly oxidise the Ti layer without overexposing it, the conductance along the wire is monitored by superimposing a 10 mV AC voltage to the DC bias of the Ti film and measuring the AC current through the device. The DC voltage is kept constant until a stable conductance is observed, indicating the maximum oxide thickness for that given voltage. As soon as the ohmic signal tends to drop below the capacitive current, oxidation is stopped. Fig. 2(b) plots the final stage of barrier formation, where the conductance changes are of the order of  $2e^2/h$ . Figure 3 shows an AFM image of a finished device. The two large oxide pads define the 70 nm wide constriction, which is then intersected by the oxide barrier. Taking a cross section along the A-B line the oxide width is measured to be 21 nm. In this way several devices with barrier widths from 15 nm to 30 nm were prepared.

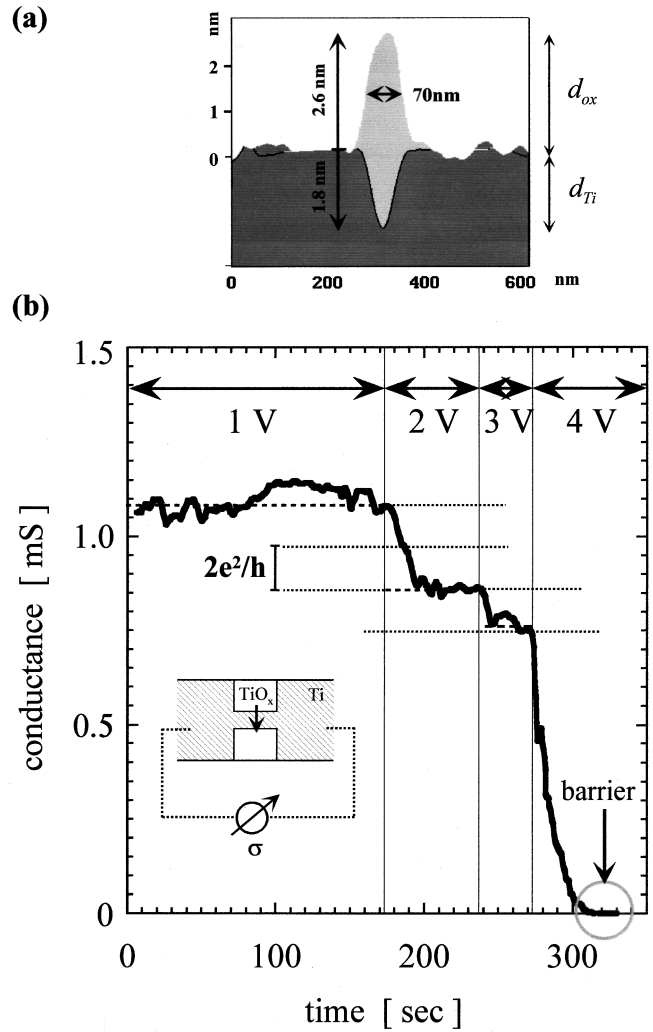


FIG. 2. *In situ* control of the barrier formation. The conductance through the device is monitored while oxidising. The tip is repeatedly scanned at a rate of 1–2 Hz. The electrical bias on the tip is increased in discrete steps (+1 V), giving the oxide time to grow. At  $t=320$  s the oxide actually forms an insulating barrier. Top: Cross section through a typical  $\text{SiO}_x/\text{Si}$  barrier.

The current-voltage ( $I$ - $V$ ) characteristic of the devices is investigated in order to test them as indeed being tunneling barriers. The 70 nm (metallic) constriction shows linear, i.e. ohmic behavior (Fig. 4). After barrier formation a change in resistance of at least four orders of magnitude is observed and the  $I$ - $V$  characteristic becomes non-linear, but asymmetric, even at room temperature. This can be explained by assuming an asymmetrical junction, which would no longer be isotropic for forward and reverse bias. This behavior is typical of all devices made and is stable in time. Thus, in contrast to  $\text{Al}/\text{Al}_2\text{O}_3$  structures,<sup>10</sup>  $\text{Ti}/\text{TiO}_x$  junctions remain in equilibrium and are therefore more practicable for applications. In order to verify the exponential dependence of the current on the barrier width, the typical behavior of the tunneling mechanism, we plot in Fig. 5 the conductance of four different devices against their barrier width as measured with AFM. This might not be the actual width of the tunneling barrier, but should be closely related to it. In fact, the current  $j_x$  depends on the oxide width  $w$  like  $j_x \propto \exp(-w \cdot \sqrt{\Phi})$ , indicating tunneling is the dominant conduction mechanism. Fitting this simplified expression to our data, a barrier height

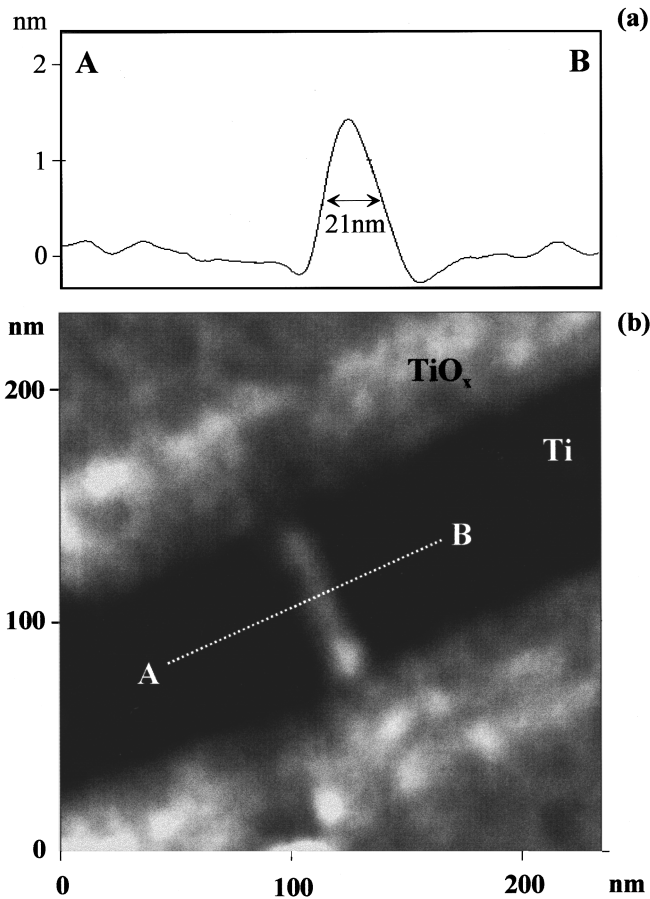


FIG. 3. AFM top view image of a Ti/TiO<sub>x</sub> barrier. The image shows the 70 nm wide metallic wire (black), defined by the AFM induced oxide and the barrier. The conductivity was monitored during formation in Fig. 2. Section A-B shows the barrier to be 21 nm wide (full width at half-maximum).

of  $\Phi = 178$  meV is estimated. A value of the same order was extracted by Matsumoto *et al.*<sup>21</sup> measuring the temperature dependence of the current.

In summary we have shown that tapping mode AFM is suitable for locally oxidising non-noble metal films. This mode significantly reduces tip degradation and, combined with an *in situ* electrical measurement, provides a highly controllable lithographic tool for fabricating nanometer-scale

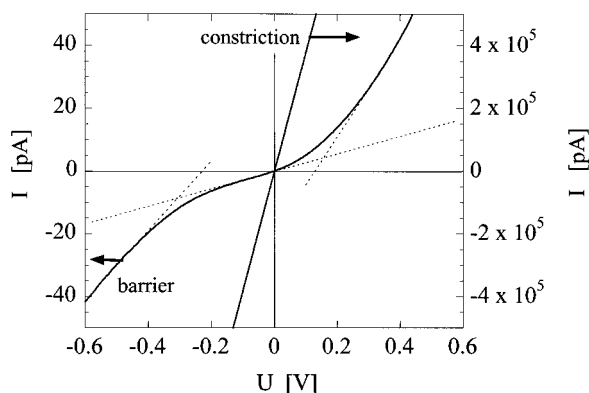


FIG. 4. IV characteristic of the 70 nm wide, AFM defined metallic wire (right axis) before barrier formation, and the 21 nm wide barrier (left axis). Dotted lines are tangents to the zero bias and high bias regions. The formation of the barrier changes the conductance of the device for at least four orders of magnitude.

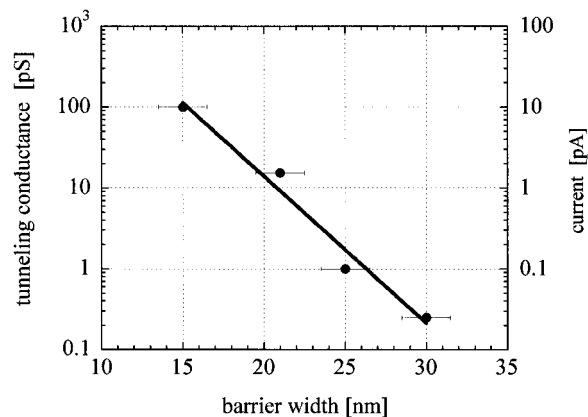


FIG. 5. A plot of the tunneling conductance vs the topographic barrier width of four different devices. The conductance depends exponentially on the barrier thickness, which clearly indicates that tunneling is the dominant conduction mechanism.

electronic devices. We demonstrated fabrication of Ti/TiO<sub>x</sub> barriers as small as 15 nm. An exponential dependence of the junction conductance of the barrier width and the I-V characteristic strongly indicate tunneling behavior.

It is a pleasure to thank M. Wendel, S. Manus, and A. Kriele for excellent collaboration. This work was supported financially by the Volkswagen-Stiftung, which is gratefully acknowledged.

- <sup>1</sup>D.M. Eigler and E.K. Schweizer, Nature (London) **344**, 524 (1990).
- <sup>2</sup>M. Wendel, S. Kühn, H. Lorenz, J.P. Kotthaus, and M. Holland, Appl. Phys. Lett. **65**, 1775 (1994).
- <sup>3</sup>E.S. Snow, P.M. Campbell, and P.J. McMarr, Appl. Phys. Lett. **63**, 749 (1993).
- <sup>4</sup>R.C. Barrett and C.F. Quate, Ultramicroscopy **42-44**, 262 (1992).
- <sup>5</sup>J. Cortes Rosa, M. Wendel, H. Lorenz, J.P. Kotthaus, M. Thomas, and H. Kroemer (unpublished).
- <sup>6</sup>J.A. Dagata, J. Schneir, H.H. Harary, C.J. Evans, M.T. Postek, and J. Benett, Appl. Phys. Lett. **56**, 2001 (1990).
- <sup>7</sup>E.S. Snow and P.M. Campbell, Appl. Phys. Lett. **64**, 1932 (1994).
- <sup>8</sup>J.W. Lyding, T.-C. Shen, J.S. Hubacek, J.R. Tucker, and G.C. Abein, Appl. Phys. Lett. **64**, 2010 (1994).
- <sup>9</sup>H. Sugimura, T. Uchida, N. Kitamura, and H. Masuhara, Appl. Phys. Lett. **63**, 1288 (1993).
- <sup>10</sup>E.S. Snow, D. Park, and P.M. Campbell, Appl. Phys. Lett. **69**, 269 (1996).
- <sup>11</sup>D. Wang, L. Tsau, and K.L. Wang, Appl. Phys. Lett. **67**, 1295 (1995).
- <sup>12</sup>Q. Zhong, D. Inniss, K. Kjoller, and V.B. Ellings, Surf. Sci. Lett. **270**, L688 (1993).
- <sup>13</sup>E.S. Snow and P.M. Campbell, Science **270**, 1639 (1995).
- <sup>14</sup>Point probes from Nanosensors GmbH, Germany.
- <sup>15</sup>M. Kehrle, A. Kriele, B. Irmer, H. Lorenz, and J.P. Kotthaus (unpublished).
- <sup>16</sup>M. Ishii and K. Matsumoto, Jpn. J. Appl. Phys., Part 1 **34**, 1329 (1995).
- <sup>17</sup>An applied external electric field of course also affects the oscillation of the cantilever. As we cannot see a significant change in the amplitude of the oscillation, but do see a mainly static deflection that causes the  $z$  piezo to withdraw the tip, the static interpretation given here seems appropriate to our experiment.
- <sup>18</sup>J. Servat, P. Gorostiza, and F. Sanz, J. Vac. Sci. Technol. A **14**, 1208 (1996).
- <sup>19</sup>The expected current flow is estimated from the oxidised volume TiO<sub>2</sub>, corresponding to the transferred charge, and typical exposure times of approximately 2 pA.
- <sup>20</sup>The cross section actually shows a Si/SiO<sub>2</sub> line, fabricated by AFM induced oxidation, because SiO<sub>2</sub>/Si can be etched far more selectively than would be possible for TiO<sub>2</sub>/Ti. The behaviour principle, however, is the same.
- <sup>21</sup>K. Matsumoto, M. Ishii, K. Segawa, and Y. Oka, Appl. Phys. Lett. **68**, 34 (1996).